

2007

Cool Flame Propagation Speeds

Michael R. Foster

George Fox University, mfoster@georgefox.edu

Howard Pearlman

Drexel University

Follow this and additional works at: https://digitalcommons.georgefox.edu/mece_fac

 Part of the [Heat Transfer, Combustion Commons](#), and the [Propulsion and Power Commons](#)

Recommended Citation

Foster, Michael R. and Pearlman, Howard, "Cool Flame Propagation Speeds" (2007). *Faculty Publications - Biomedical, Mechanical, and Civil Engineering*. 28.
https://digitalcommons.georgefox.edu/mece_fac/28

This Article is brought to you for free and open access by the Department of Biomedical, Mechanical, and Civil Engineering at Digital Commons @ George Fox University. It has been accepted for inclusion in Faculty Publications - Biomedical, Mechanical, and Civil Engineering by an authorized administrator of Digital Commons @ George Fox University. For more information, please contact arolfe@georgefox.edu.

Cool Flame Propagation Speeds

Michael Foster and Howard Pearlman*

Department of Mechanical Engineering and Mechanics, Drexel University,
Philadelphia, USA

Abstract: Cool flames are studied at reduced-gravity in a closed, unstirred, spherical reactor to minimize complexities associated with natural convection. Under such conditions, transport is controlled by diffusive fluxes and the flames are observed to propagate radially outward from the center of the reactor toward the wall. Intensified video records are obtained and analyzed to determine the flame radius as a function of time for different vessel temperatures (593–623 K) and initial pressures (55.2–81.4 kPa) using an equimolar ($\phi = 5$) propane-oxygen premixture. Polynomial-fits are applied to the data and differentiated to determine the cool flame propagation speeds. In nearly all cases considered, the flame decelerates monotonically and in some cases, subsequently retreats towards the center of the reactor. The flame speed is also tabulated as a function of the flame stretch rate. Extrapolation of the cool flame speeds to zero stretch is then performed to determine the “unstretched” cool flame propagation speeds.

Keywords: Cool flames; Flame speed; Low-temperature combustion; Reduced-gravity

INTRODUCTION

At low ($T < 650$ K) and intermediate temperatures (650 K $< T < 1000$ K), cool flames and multi-stage ignitions occur in many aliphatic hydrocarbon fuel-air mixtures for which the chemistry is dominated by reactions that

Received 7 July 2006; accepted 16 November 2006.

Special thanks are offered to the NASA KC-135 crew, pilots and support staff. This work was funded by NASA grant NCC3-1008 and NSF GRFP.

*Address correspondence to hp37@drexel.edu

involve propylperoxy and hydroperoxy radicals. At higher temperatures, production of hydrogen peroxide and its subsequent decomposition to hydroxyl radicals $\text{HO}\bullet$ becomes increasingly important and leads to hot ignition. To refine the chemical kinetic mechanisms associated with hydrocarbon oxidation and understand the shifts in the temperature-dependent pathways, many studies have been conducted with alkanes, alkenes, and aromatics in different configurations. These include unstirred, static reactors, continuously-stirred tank reactors (CSTR's), pressurized-flow reactors, and rapid compression machines (Pease, 1929; Newitt and Thornes, 1937; Seakins et al., 1963; Gray and Felton, 1974; Wilk et al., 1986; Koert et al., 1994; Curran et al., 1996). A comprehensive review of experimental and numerical studies performed with different fuels at low and intermediate temperatures is given by Griffiths and Mohamed (1997).

In closed stirred and CSTR studies, natural convection and diffusive transport are suppressed to minimize spatial gradients and focus attention on the physical chemistry of the problem (Griffiths, 1985; Griffiths and Scott, 1987; Gray and Scott, 1990; Faravelli et al., 1998). However, hydrodynamics and diffusive transport have long been recognized to play important roles in all unstirred cool flame and multi-stage ignition studies (Fine et al., 1970; Griffiths et al., 1970; Barnard and Harwood, 1974; Pearlman, 1999; Fairlie et al., 2005). Also, numerical studies of thermokinetic oscillations and ignitions in closed reactors have recently begun to include natural convection and diffusive transport (Campbell et al., 2005, 2006).

As such, the present study considers the reactive-diffusive cool flame structure and its spatio-temporal evolution in a closed, static reactor when transport is governed solely by diffusive fluxes and natural convection can be disregarded. Such conditions exist in a reduced-gravity environment in which the Rayleigh number is sufficiently small (Pearlman, 1999). Specific attention is given to the propagation speeds associated with cool flames in a rich equimolar propane-oxygen premixture to provide the first benchmark experimental data on diffusion-controlled cool flame propagation speeds to further validate chemical kinetic mechanisms at low and intermediate temperatures. Propane is selected since it is the simplest alkane that exhibits a Negative Temperature Coefficient (NTC) behavior (Pease, 1929, 1938; Day and Pease, 1940).

EXPERIMENTAL APPARATUS

A Mallard-Le Chatelier static, unstirred reactor is used to conduct the experiments. The reactor is a fused-silica spherical vessel (i.d. = 10.2 cm, wall thickness = 3 mm) housed in a box furnace (maximum temperature of 873 K). The vessel is initially preheated and evacuated to 2.7 Pa (0.02 Torr) or below as determined with a vacuum thermocouple gauge.

The furnace temperature is monitored with a 0.020" type-K thermocouple. An equimolar premixture of propane and oxygen is prepared by partial pressure gas mixing and stored in 300 cc stainless-steel, gas cylinders prior to testing.

The reactor pressure is monitored with a Setra Model 204 0–172 kPa pressure transducer (absolute accuracy: ± 0.19 kPa) mounted on the gas inlet (cold side) of the reactor. Intensified video cameras image the reaction from the top (oriented downward) and the side (orthogonal to the top camera) of the furnace. The side camera is a Hamamatsu model C5909 ICCD camera and the top camera is a Dalsa/SMD ICCD-1M30P camera equipped with a fiber-coupled 18 mm Gen II UV image intensifier. Both cameras are operated at maximum gain and image the reactor through three 3.2 mm thick, 6.4 cm diameter quartz windows spaced 1.27 cm apart used to minimize heat loss and improve temperature uniformity within the furnace. Standard framing rates of 30 frames per second are obtained.

The furnace with reactor, premixed gas mixing and delivery system, and vacuum pump are mounted aboard NASA's KC-135 reduced-gravity aircraft and tests are conducted during free-fall maneuvers between 32 kft and 24 kft. The reaction is monitored during the 20–23 s descent. Figure 1 shows a typical acceleration history detailing the normalized x, y, and

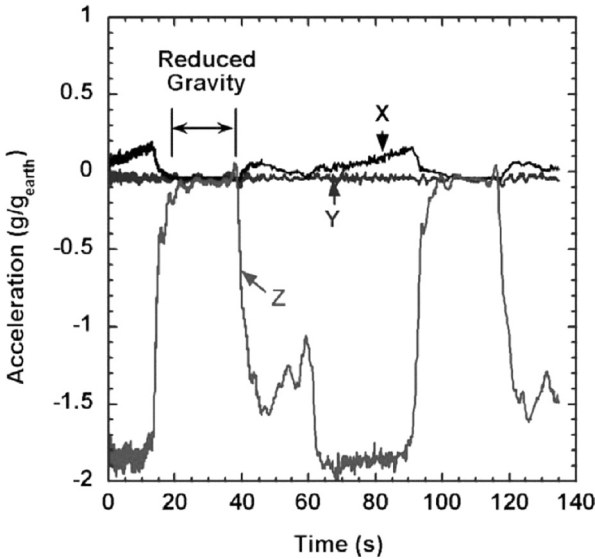


Figure 1. Representative NASA KC-135 reduced-gravity aircraft acceleration profiles obtained during free-float parabolic maneuvers. Acceleration values are normalized by Earth's gravitational acceleration.

z-components of acceleration as determined with a three-axis $\pm 2g$ accelerometer, where the x and y components correspond to the horizontal plane and z corresponds to the vertical plane relative to the aircraft. All components of acceleration are approximately one-hundredth of Earth's gravity during free-fall, albeit accompanied by high-frequency oscillations due to mechanical vibrations and aerodynamic stresses on the aircraft. Each test begins by filling a pre-evacuated 50 cc stainless-steel sample cylinder to appropriate pressure. This 50 cc cylinder is separated from the reactor by a pneumatic, vacuum-tight solenoid valve. Once near-zero gravity conditions are achieved as determined by the accelerometer, the solenoid valve is opened and the vessel is filled to a prescribed initial pressure. The solenoid valve is then closed and the reactor is isolated.

EXPERIMENTAL RESULTS

Intensified Imaging and Image Analysis

At reduced-gravity, the associated Rayleigh number (Ra) is on the order of 10^3 (or less), within the error bar (± 500) of the empirical value needed to suppress natural convection in a spherical reactor ($Ra_{critical} \approx 600$) (Tyler, 1966; Fine et al., 1970; Griffiths et al., 1970).

A typical sequence of propane cool flame images is shown in Figure 2 taken with the side camera at 68.9 kPa and 613 K. For these conditions, the cool flame shown is the first stage of a two-stage ignition as seen in the corresponding pressure history shown in Figure 3. Note that frames (a)–(e), which are visible cool flames, occur in the circled region of the pressure history.

Using a commercially available image analysis software program (Igor Pro), line intensity profiles are taken vertically at two different horizontal locations equidistant from the flame centerline and the average horizontal pixel intensity value at each vertical position is tabulated as

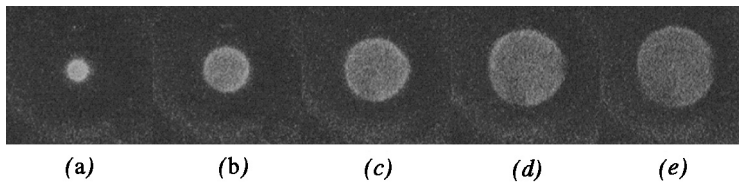


Figure 2. Cool flame in an equimolar propane-oxygen premixture at 68.9 kPa and 613 K at reduced-gravity. Time between frames is 1/3 s. Image contrast enhanced for clarity.

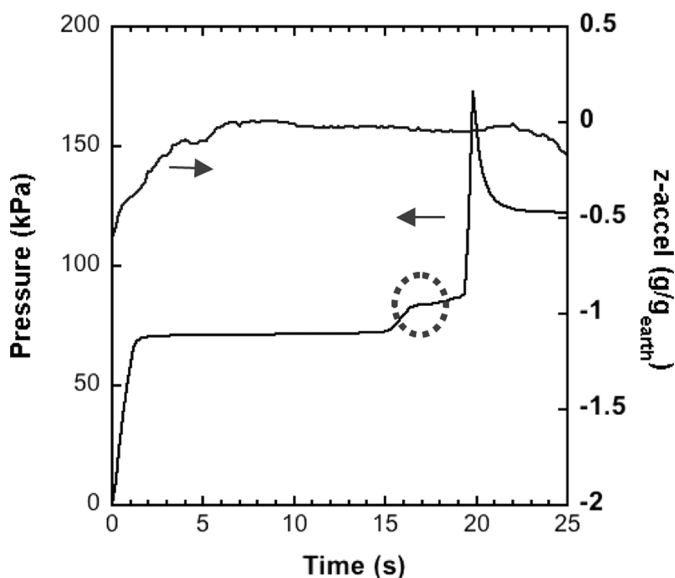


Figure 3. Pressure history associated with the cool flame shown in Figure 2. Dotted region indicates range of pressures during which visible light emission shown in Figure 2 is observed.

shown in Figure 4. Line-averaging reduces the intensifier Schott noise in the video data. The flame location is then defined as the location associated with a 63% rise in the intensity value above the background noise floor relative to the peak intensity value for each frame. A 7-point averaging scheme (repeated three times) in addition to a 19-point least-squares method is also used to smooth the experimental intensity value data. To resolve line-of-sight integration errors, a three-point Abel deconvolution is then applied to the smoothed data. The estimated error bar on all reported radius values due to data analysis and post processing is ± 2.5 mm (± 14 pixels).

A third-order polynomial fit is then applied to the flame radius (R_f) data, differentiated, and used to determine the cool flame propagation speed ($V_f = dR_f/dt$) as a function of time. Figures 5a-d show R_f and V_f as functions of time for different initial reactant pressures and wall temperatures (T_w) equal to 593 K, 603 K, 613 K, and 623 K, respectively. In each figure, $t = 0$ s corresponds to the initial flame radius obtained from the first discernable video frame. It is noted that these reactive-diffusive cool flames are not simply phase waves where different regions oscillate at different phases; diffusive fluxes do play a significant role (Fairlie et al., 2005). For the cool flames considered, the chemical times are on the order of seconds (or longer) and not significantly shorter than

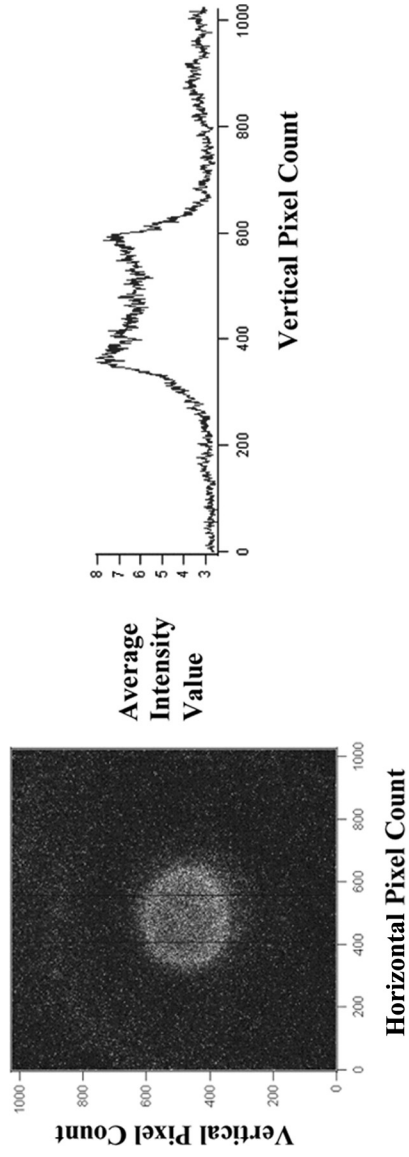


Figure 4. Representative cool flame image and spatially-averaged line intensity profile (5.9 pixels = 1 mm). Note that the internal walls of the reactor are at 168 and 768 pixels. In this test, $T_w = 613\text{ K}$, $P_{\text{initial}} = 66.9\text{ kPa}$, $\phi = 5$.

the diffusion times. Estimates of the thermal and mass diffusion times given by R^2/α and $R^2/D_{C_3H_8-O_2}$, are 42 s and 34 s, respectively. Note that the diffusion coefficients ($\alpha = 61.4 \text{ mm}^2/\text{s}$ and $D_{C_3H_8-O_2} = 76.7 \text{ mm}^2/\text{s}$) were computed for an equimolar propane-oxygen mixture at 600 K and 50.6 kPa.

Also note that in all cases tested, the cool flame originates at (or near) the center of the reactor and then decelerates as it propagates radially outward towards the wall. Each curve corresponds to a separate parabolic free-fall test aboard NASA's reduced-gravity aircraft. In some cases, the cool flame approaches the wall, stops expanding outwardly and reverses direction as the location of the peak intensity retreats towards the center of the reactor. Such behavior is indicated in Figure 5 by *negative* flame speeds and has been observed numerically by Fairlie and co-workers (Fairlie et al., 2005). Also note that the peak light intensity decreases monotonically during the course of the flame propagation.

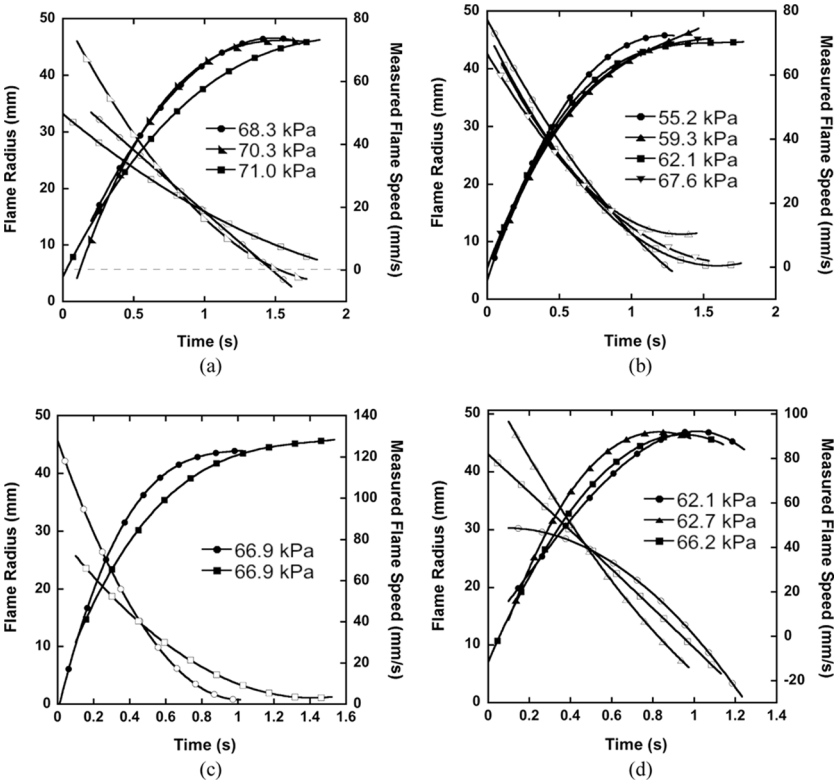


Figure 5. Flame radius (closed symbols) and flame speed (open symbols) versus time for different initial reactor pressures at fixed wall temperatures: $T_w =$ (a) 593 K, (b) 603 K, (c) 613 K, (d) 623 K.

Flame Stretch

Spherically expanding reactive-diffusive cool flames are expected to be affected by curvature and flow strain effects, i.e., flame stretch, in much the same manner as spherically expanding premixed gas flames. Flame stretch, a measure of the relative rate change of the flame front area (Karlovitz et al., 1953), is given as $\kappa = 2V_f/R_f$ for spherically-expanding flames (Matalon, 1983; Law, 1988).

As a first step towards understanding stretch effects on cool flames, Figures 6a–d plot the experimentally measured cool flame speeds versus stretch rates for four different temperatures for different pressures. In all cases, an exponential rise is observed. Near-zero values of the stretch rate correspond to the cases when the cool flame resides in the vicinity of the wall and negative values correspond to the cases when the cool flame retreats radially inward. Note also that the values of flame stretch are relatively small compared to those associated with high-temperature premixed gas combustion, due to the significantly smaller cool flame propagation speeds.

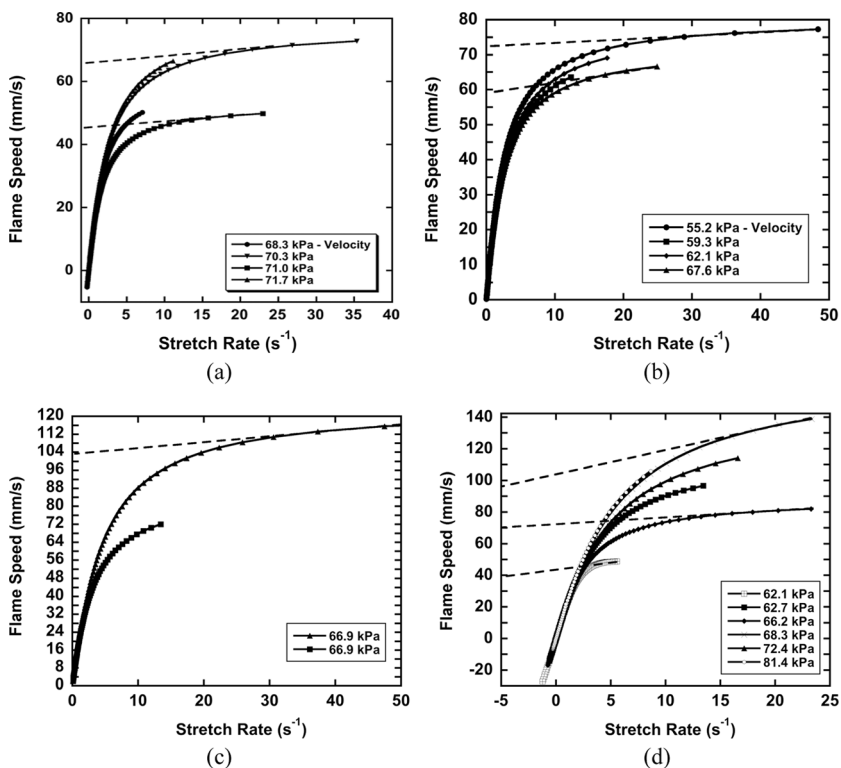
At present, an expression that incorporates the effects of curvature, heat loss, thermal expansion, and Lewis number on laminar cool flame speeds does not exist as it does for premixed gas flames (Ronney and Sivashinsky, 1989). While a recent two-step Sal'nikov model augmented with diffusive transport (Fairlie et al., 2002) suggests that cool flame oscillations damp as Le increases (for $Le \geq 1$), the Sal'nikov mechanism is purely based on thermal feedback, not chain-thermal feedback that is characteristic of hydrocarbon oxidation and cool flames. Also, parallels with spherically expanding flames suggest that a linear relation between flame speed and flame stretch rate is appropriate for flames with moderate curvature and strain rates (Markstein, 1964; Clavin, 1985), i.e., $V_f = V_f^0 - L\kappa$ where V_f^0 is the unstretched, laminar burning velocity, L is the Markstein length and κ is the flame stretch rate. If a linear fit is applied in the early and intermediate stages of the cool flame evolution, prior to significant wall losses, the slope of the line L is negative as the flame speed increases with increasing positive stretch rate; this suggests the flames are unstable. Heat loss and preferential diffusion may provide stabilizing mechanisms.

From the linear extrapolations, the unstretched laminar cool flame propagation speeds for select temperatures and pressures are summarized in Table 1. For the two cases extrapolated at 593 K shown in Figure 6a, the dependence of flame speed on flame stretch (i.e., L) is approximately the same. At 603 K, L increases weakly with increasing pressure, while only two data sets were obtained at 613 K for 66.9 kPa due to the limited availability of NASA's KC135 aircraft. For this temperature and pressure, repeatability was questionable, which can perhaps be attributed to errors

Table 1. Unstretched cool flame propagation speeds

T (K)	P (kPa)	V_f unstretched (mm/s)
593	71.0	46
593	70.3	66
603	55.2	60
603	67.6	72
613	66.9	103
623	62.1	40
623	66.2	70
623	68.3	96

associated with residual gas impurity between sequential tests, gas entry effects, and g-jitter (the time-dependent variation in the acceleration due to mechanical and aerodynamically induced vibrations). Furthermore, at 623 K, L has a nonlinear dependence on pressure as it increases from

**Figure 6.** Flame stretch as a function of flame speed for different initial temperatures: (a) 593 K, (b) 603 K, (c) 613 K, (d) 623 K.

62.1 kPa to 62.7 kPa, decreases from 62.7 kPa to 66.2 kPa and then increases, decreases and increases yet again with increasing pressure.

Comparison with Numerical Prediction of Light Emission from Excited Formaldehyde

Currently, the only model appropriate for propane oxidation at low and intermediate temperatures that includes diffusive fluxes of heat and species has been recently reported by Fairlie and co-workers (2005). Using the EXGAS detailed chemical kinetic model (Warth et al., 1998) appropriate for propane in the temperature range 600–2000 K, a reduced mechanism with 58 species and 378 reactions was developed, extended to include diffusion of heat and species, and solved numerically. While shown to be more reactive than the experimental data, an increase in the radius of the peak light emission from excited formaldehyde was predicted followed by a slight retreat of the peak intensity towards the center of the reactor, at least in the case of 593 K and 46.7 kPa (Fig. 3 of Fairlie et al., 2005). Qualitatively, the trend is similar to the experiments conducted at 68.3 kPa and 70.3 kPa at 593 K shown in Figure 5a. To further validate the mechanisms and refine the rate constants, if needed, additional numerical computations and higher fidelity experiments with species concentration measurements are obviously needed.

CONCLUSIONS

Experimental data on cool flame radius and cool flame propagation speeds are reported for propane oxidation under pure diffusive conditions. The flames decelerate as they propagate radially from the center towards the walls and in select cases, the peak intensity subsequently moves inwards towards the center. Qualitatively, a similar dependence is predicted by a recently reported reduced propane oxidation mechanism (Fairlie et al., 2005). Additionally, the first plots of cool flames speed versus flame stretch are reported showing the flame speed increases with increasing stretch rate. A linear fit for select cases is then used to extrapolate the unstretched cool flame propagation speeds for the temperatures and pressures considered.

REFERENCES

- Barnard, J.A. and Harwood, B.A. (1974) Physical factors in the study of the spontaneous ignition of hydrocarbons in static systems. *Combust. Flame*, **22**, 35–42.

- Campbell, A., Cardoso, S., and Hayhurst, A. (2005) A scaling analysis of Sal'nikov's reaction, $P \rightarrow A \rightarrow B$, in the presence of natural convection and the diffusion of heat and matter. *Proc. Royal Soc. A: Math., Phys. Eng. Sci.*, **461**(2059), 1999–2020.
- Campbell, A., Cardoso, S., and Hayhurst, A. (2006) The behavior of Sal'nikov's reaction, $P \rightarrow A \rightarrow B$, in a spherical batch reactor with the diffusion of heat and matter. *Phys. Chem. Chem. Phys.* **8**(24), 2866–2878.
- Clavin, P. (1985) Dynamic behavior of premixed flame fronts in laminar and turbulent flows. *Prog. Ener. Combust. Sci.*, **11**, 1–59.
- Curran, H., Pitz, W., Westbrook, C., Griffiths, J., and Mohamed, C. (1996) Kinetic Modeling of Hydrocarbon Autoignition at Low and Intermediate Temperatures in a Rapid Compression Machine, 3rd Workshop on Modeling of Chemical Reaction Systems, Heidelberg, Germany, July 24–26.
- Day, R.A. and Pease, R.N. (1940) The effect of surface on cool flames in the oxidation of propane. *Proc. Roy. Soc. Lond.*, **62**, 2334–2337.
- Fairlie, R. and Griffiths, J. (2002) Oscillatory combustion in closed vessels under microgravity. *Math. Comp. Mode.*, **36**, 245–257.
- Fairlie, R., Griffiths, J., Hughes, J., and Pearlman, H. (2005) Cool flames in space: Experimental and numerical studies of propane combustion. *Proc. Comb. Instit.*, **30**, 1057–1064.
- Faravelli, T., Gaffuri, P., Ranzi, E., and Griffiths, J. (1998) Detailed thermo-kinetic modelling of alkane autoignition as a tool for the optimization of performance of internal combustion engines. *Fuel*, **77**(3), 147–155.
- Fine, D.H., Gray, P., and MacKinven, R. (1970) Thermal effects accompanying spontaneous ignitions in gases; I. An investigation of the heating effects which accompany the rapid admission of an inert gas to an evacuated vessel. *Royal Soc. Lond.*, **A**, **316**, 223–240.
- Gray, B.F. and Felton, P.G. (1974) Low-temperature oxidation in a stirred reactor—I. Propane. *Combust. Flame*, **23**, 295–304.
- Gray, P. and Scott, S. (1990) Experimental systems 2: Gas-phase reactions. In *Chemical Oscillations and Instabilities: Non-linear Chemical Kinetics*, Vol. 21 of International Series of Monographs on Chemistry, Ch. 15. Oxford University Press, Inc., New York.
- Griffiths, J. (1985) Thermokinetic oscillations in homogeneous gas-phase oxidations. In Field, R. and Burger, M. (Eds.) *Oscillations and Traveling Waves in Chemical Systems*, John Wiley & Sons, New York.
- Griffiths, J.F., Gray, B.F., and Gray, P. (1970) Multistage ignition in hydrocarbon combustion: Temperature effects and theories of non-isothermal combustion. *Proc. Combust. Instit.*, **13**, 239–248.
- Griffiths, J.F., Gray, P., and Kishore, K. (1974) The measurement of heat-loss rates from a stirred reactor using thermo-chemical method. *Combust. Flame*, **22**, 197–207.
- Griffiths, J. and Mohamed, C. (1997) Experimental and numerical studies of oxidation chemistry and spontaneous ignition phenomena, Chapter 6 in Pilling (Ed.) *Low-Temperature Combustion and Autoignition*, Elsevier Science, **35**, pp. 545–653.
- Griffiths, J. and Scott, S. (1987) Thermokinetic interactions: Fundamentals of spontaneous ignition and cool flames. *Prog. Ener. Combust. Sci.*, **13**, 161–197.

- Karlovitz, B., Denniston, D., Knapschaefer, D., and Wells, H. (1953) Studies on turbulent flames A. Flame propagation across velocity gradients. *Proc. Combust. Instit.*, **4**, 613–620.
- Koert, D., Miller, D., and Cernansky, N. (1994) Experimental studies of propane oxidation through the negative temperature coefficient region at 10 to 15 atmospheres. *Combust. Flame*, **96**, 34–49.
- Law, C.K. (1988) Dynamics of stretched flames. *Proc. Combust. Instit.*, **22**, 1381–1402.
- Matalon, M. (1983) On flame stretch. *Combust. Sci. Technol.*, **31**, 169–182.
- Markstein, G. (1964) *Non-Steady Flame Propagation*, Pergamon, New York.
- Newitt, D.M. and Thornes, L.S. (1937) The oxidation of propane, Part 1: The products of the slow oxidation at atmospheric and at reduced pressures. *J. Chem. Soc.*, 1656.
- Pease, R. (1929) Characteristics of the nonexplosive oxidation of propane and the butanes. *J. Amer. Chem. Soc.*, **51**, 1839–1856; Peace, R.N. (1938) *J. Amer. Chem. Soc.*, **60**, 2244.
- Pearlman, H. (1999) The role of buoyant convection on cool flames and low-temperature reactions. *Combust. Flame*, **121**(1–2), 390–393.
- Ronney, P. and Sivashinsky, G. (1989) A theoretical study of propagation and extinction of nonsteady spherical flame fronts. *SIAM J. Appl. Math.*, **49**(4), 1029–1046.
- Seakins, M. and Hinshelwood, C. (1963) Some correlations in the kinetics of gas-phase hydrocarbon oxidations. *Proc. Royal Soc. Lond.*, **A276**, 324–345.
- Tyler, B. (1966) An experimental investigation of conductive and convective heat transfer during exothermic gas phase reactions. *Combust. Flame*, **10**, 90–91.
- Warth, V., Battin-Leclerc, F., Fournet, R., Glaude, P.A., Côme, G.M., and Scacchi, G. (1998) Computer tools for combustion kinetic modeling. (www.ensic.u-nancy.fr/DCPR/Anglais/GCR/software.htm).
- Wilk, R., Cernansky, N., and Cohen, R. (1986) The oxidation of propane at low and transition temperatures. *Combust. Sci. Technol.*, **49**, 41–78.